Experimental and DFT Study of the Partial Oxidation of Benzene by N_2O over H-ZSM-5: Acid Catalyzed Mechanism

Pierre M. Esteves[†] and Benoît Louis*[,‡]

Instituto de Química, Universidade Federal do Rio de Janeiro (UFRJ), Cidade Universitária−Ilha do Fundão, Centro de Tecnologia-Bloco A, Rio de Janeiro-RJ, 21949-900, Brazil, and Laboratoire des Matériaux (Part of European Laboratory of Catalysis and Surface Science), Surfaces et Procédés pour la Catalyse (LMSPC, UMR 7515), ECPM-ULP, 25, rue Becquerel, F-67087 Strasbourg Cedex 2, France

Received: May 3, 2006; In Final Form: July 4, 2006

The reaction mechanism for hydroxylation of benzene by N_2O has been studied on chemically modified ZSM-5 catalysts. A maximum in catalytic activity and selectivity was reached for steamed samples under mild conditions (about 30% conversion with 94% selectivity). Chemical modifications, through ion exchange (H^+ versus Na^+), have demonstrated the importance of the presence of Brönsted acid sites. The results obtained suggest a Langmuir−Hinshelwood mechanism between benzene and N_2O adsorbed on two distinct active sites. A density functional theory study considering the possible reaction intermediates also confirmed the possible formation of protonated nitrous oxide, leading to a Wheland-type intermediate, thus supporting an electrophilic aromatic substitution assisted by the confined environment provided by the active zeolite framework.

Introduction

Partial oxidation of aromatics is one of the most challenging reactions in the field of organic synthesis.[1,2] The actual cumene process has the main drawback of producing phenol in a three-step synthesis; its efficiency is mainly due to the valuable market price of the byproduct acetone. Therefore, efforts to develop a new way to produce phenol (Alphox Solutia process) through a one-step synthesis are undertaken. Several attempts to perform the one-step reaction with molecular oxygen failed, since carbon dioxide was the only product formed. Alternative oxidants were tested in the direct hydroxylation, such as H_2O_2[3,4] or O_3 in superacid media.[5]

Iwamoto et al. have introduced N_2O as oxidant, which opened a new opportunity for the gas-phase phenol synthesis.[6] Suzuki et al. have obtained a 90% selectivity toward phenol by using N_2O and H-ZSM-5 zeolite as catalyst.[7] Since the past decade, this reaction is known to proceed between 300 and 400 °C on ZSM-5-type catalysts with selectivity close to 100%.

Unfortunately, the chemical nature of the active sites and the reaction mechanism are still unclear. Some authors suggested that only Brönsted acidity was responsible of the catalytic activity.[7−9] Conversely, Panov and co-workers found evidence for the participation of small iron clusters in the catalysis of this reaction.[10−13] They claimed that iron centers (α-sites) are necessary to decompose N_2O in N_2 and that an active surface species, so-called α-oxygen, is responsible for the phenol formation in a biomimetic manner, acting like enzyme monooxygenases.[10−13]

Recently, several research groups have related the zeolite activity to Lewis acid sites formed by coordinately unsaturated aluminum species present in the channels of the lattice.[14−17] It is well-demonstrated in the literature that extraframework aluminum (EFAl) species formed during chemical, thermal, or hydrothermal treatment are responsible for an enhancement of the zeolites activity in many acid-catalyzed processes.[18−26]

Selectivity toward phenol can be increased by thermal and hydrothermal treatment, which is known to dealuminate the zeolite framework.[22−26] Dealumination proceeds through a release of Al from the zeolite lattice to form Lewis EFAl, which stays in the channels of the ZSM-5 zeolite structure. Despite the lack of knowledge of their exact nature and of their involvement in the reaction, two general possibilities exist: (a) EFAl species can be itself a catalytic site and (b) EFAl can interact with framework Al, stabilizing the negative charge of the framework and thus increasing the strength of neighboring protons and creating "superacid sites" by this association.[27]

The special geometry of the ZSM-5 structure, with its well-structured microporous network, is able to stabilize small metal complexes.[28] Furthermore, the electrostatic environment of the ZSM-5 matrix, due to the presence of aluminum and counterions, guide the reactants toward the active sites by electrostatic interaction.[29−34] This can also favor the stabilization of carbocationic intermediates.[35−39] The zeolite framework can therefore act as a solid solvent that absorbs before adsorbing the reactants.[32,33]

The present work reports the influence of different modifications of the ZSM-5 zeolite, either by steaming−calcination or by chemical modification, on the benzene partial oxidation by N_2O. Our aim is to study the influence of the Brönsted and Lewis acidity, separately and together in this reaction. In this context, the issue whether an (super)acid-catalyzed pathway might be an alternative to the iron-mediated process was also investigated by means of DFT calculations.

Experimental Details

Catalyst Preparation. The H-ZSM-5 zeolite (Zeocat PZ-2/50-H) was provided by Zeochem, Switzerland. This zeolite was chosen for different chemical modifications:

* Corresponding author. E-mail: blouis@chimie.u-strasbg.fr.
[†] Universidade Federal do Rio de Janeiro.
[‡] ECPM-ULP.

10.1021/jp062715f CCC: $33.50
Published on Web 08/01/2006

TABLE 1: Composition and Properties of the Materials

catalyst	Si/Al	SSA (m^2/g)	pore volume (cm^3/g)
Zeochem (PZ/50H)	25	335	0.317
HCl-Zeochem	52	435	0.762
TEOS-Zeochem	33	259	0.292
H[F]-ZSM-5	41	358	0.267

Back-Exchange: H^+ for Na^+. Prior to the exchange procedure, the catalyst was activated at 773 K for 2 h in air. Then, 6 g of extrudated pellets was impregnated in a 100 mL solution of sodium methanolate in THF (0.1 M) at 323 K for 3 h (anhydrous conditions). Afterward, the catalyst was filtered and thoroughly washed with THF and dried at 453 K. Finally, the material was calcined at 823 K for 15 h in air.

Leaching with Hydrochloric Acid. The H-form of the zeolite was treated with an aqueous hydrochloric acid (32 wt %) solution at 323 K for 4 h as already reported.[9] After cooling to room temperature, the solution was maintained at 273 K for 2 h. After washing with demineralized water, the zeolite was dried at 373 K overnight.

TEOS Treatment. To selectively passivate the acid sites of the outer surface, the sample was impregnated for 15 h by a solution of tetraethyl orthosilicate (TEOS) in dry hexane. The sample was then dried at 393 K for 3 h and subsequently calcined in air at 823 K for 5 h in order to remove the organic compounds

Steaming and Calcination. In the case of hydrothermal treatment, the catalyst was steamed at 823 K under a water partial pressure of 310 mbar. The duration of steaming has been varied in order to evaluate its influence on the catalytic properties. For comparison purposes, in the catalytic performance, the catalyst was simply calcined in air at 973 K for 2 h.

Synthesis of H[F]-ZSM-5. The mole ratio of the reactants was as follows: TPA-Br:TEOS:$NaAlO_2$:NH_4F:H_2O = 0.07:1:0.012:(0.3−1.6):80 as reported elsewhere.[40] The pH was adjusted to 7 by adding a few drops of hydrofluoric acid solution (40 wt %). The gel was then poured into an autoclave and kept for 135 h at 443 K. The crystalline material was filtered, washed with demineralized water, and dried at 393 K. The H-forms were obtained by 5 h calcination at 773 K in air. The chemical composition of all these materials and their sorption properties are given in Table 1.

Characterization. Specific surface areas (SSA) of the catalysts were determined by nitrogen adsorption (77 K) by employing the BET method via a Sorptomatic 1900 (Carlo-Erba). X-ray diffraction (XRD) patterns of powdered catalysts were determined on a Siemens D500 diffractometer with Cu Kα monochromatic radiation (λ = 1.5406 Å). The Si/Al ratios of the crystals were determined by energy-dispersive X-ray (EDX) analysis coupled with the SEM chamber.

The chemical composition of the samples was either determined by XPS spectroscopy (PHI-550 ESCA-system, Perkin-Elmer GmbH) or by atomic absorption spectroscopy (AAS, AA-1100, Perkin-Elmer GmbH).

Setup and Procedure. The catalytic reaction was carried out at 623 K and atmospheric pressure in a stainless steel tubular reactor. The catalyst (5 g) was placed in the middle part of the reactor between two glass beads zones. The activation of the catalyst was either performed by steaming or calcination in air. The reaction mixture contained 4 mol % of benzene and 16 mol % of N_2O; nitrogen was used as diluent. The total flow was set to 100 mL STP/min. Aromatics were analyzed by GC on-line (Shimadzu GC-14A, 30 m HP-5, FID). The CO_2 formation was monitored by an IR analyzer (Siemens Ultramat-22P).

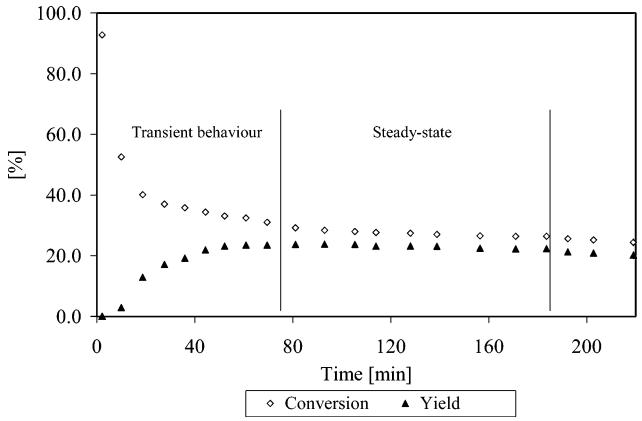

Figure 1. Reaction profile for the catalytic reaction

A considerable loss in activity during the reaction was observed due to catalyst coking. Therefore, the conversion (quantity of benzene having reacted) and phenol yield were only measured after 1 h on stream, since at this point steady-state was reached (Figure 1). The phenol yield was calculated in terms of the quantity of phenol formed from the initial amount of benzene introduced in the reactor.

The catalyst regeneration was performed overnight under a flow of air at 773 K, and the initial activity could be restored. The reaction conversion was calculated from the quantity of the reacted benzene. The selectivity toward phenol was defined as the mole ratio of the phenol formed to the benzene converted.

Results and Discussion

Results on Benzene Partial Oxidation. Characterization. AAS measurements showed that Zeochem parent catalyst contains an iron content between 0.06 and 0.1 wt %. As-synthesized [F]-ZSM-5 has only an iron content of 0.02 wt %. Table 1 shows the chemical properties of the different zeolites. Before modification, the Zeochem catalyst presented almost the same SSA and pore volume values than the H[F]-ZSM-5 catalyst. The former showed an increase from 25 to 52 for the Si/Al ratio after hydrochloric acid treatment. This is not surprising, since mineral acids are commonly used for the dealumination of zeolites. Leaching of zeolitic materials with HCl removes a large number of aluminum atoms from the framework and extraframework, through a coordination−dissolution mechanism.[30] Furthermore, both SSA and pore volume were increased, thus indicating the formation of mesopores (hysteresis loop at P/P_0 between 0.2 and 0.4).

TEOS-treated sample presents a large decrease in the SSA value (about 80 m^2/g); this corresponds to the selective passivation of the zeolite outer surface via silanization. Due to the small size of the pores in ZSM-5 (i.e., large size of TEOS), only silanization of the outer surface is achieved. This high SSA of the external surface (ESA) gives precious information on the ease of dealumination; it has been demonstrated that the level of dealumination is usually higher for samples with larger ESA values.[41]

The XRD powder patterns confirmed that the crystallinity remained unchanged for all chemically modified MFI materials.

The characteristics of the H[F]-ZSM-5 materials were reported in our previous study.[40] However, XPS measurements after calcination steps confirmed the presence of fluoride anion

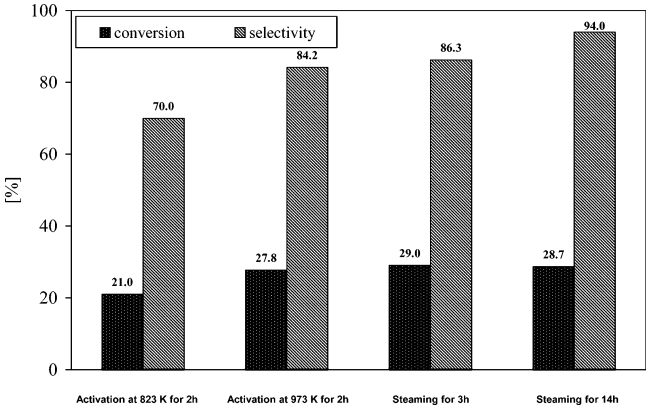

Figure 2. Dependence between the activation procedure and the catalyst activity and selectivity.

inside the zeolite lattice (1.6 wt %). Fluorine is known to modify the surface composition,[42−43] thus influencing the catalytic properties.

Acid−Base Properties. The amount of Brönsted acid sites tends to decrease while introducing fluoride anions in the synthesis gel, as already observed after a study of TPD of pyridine.[40] For instance, the zeolite sample with F/Si = 1.6 and having a Si/Al = 41 should possess a theoretical amount of Brönsted acid sites of 0.4 mmol H^+/g zeolite. The measured value for this sample was about 0.05 mmol H^+/g zeolite. The strength of these remaining sites has also been shown to be lower when compared to the zeolite synthesized under basic conditions.[40] Thus, the fluoride anions really present a detrimental effect both on the number and strength of the Brönsted acid sites.

Hölderich et al. have shown the formation of EFAl species[14] by FT-IR measurements, under the same steaming conditions and using the same commercial zeolite. After 3 h of steaming, the frequency of the asymmetrical Si−O−Al stretching vibration showed an increase of 4 cm^{-1} toward higher values. This shift toward higher wavenumbers is an undoubtedly proof of the dealumination of the lattice.[14,15] Moreover, nonframework Al species usually exhibit Lewis acidity. Second, the steaming led to EFAl formation, known to increase the acid strength of the remaining neighboring Brönsted acid sites.[19,24,27] Moreover, while exchanging the zeolite by Na^+ cations, a complete depletion of Brönsted acid sites could be observed by TPD of pyridine.

In summary, we have prepared several samples presenting different kinds of acidity: Brönsted acidity (BA), Brönsted and exhibited Lewis acidity (LA), reduced BA (both in number and strength), and reduced Lewis acidity. Despite the fact that there is no doubt that iron centers, presumably binuclear complexes,[10−13,28,44,45] can activate N_2O molecules and generate α-oxygen species, our samples possess a relatively low amount of iron, which raises the subject of whether acid sites can by themselves catalyze the same reaction. To address this point we have compared their activity to H[Fe]-ZSM5 prepared according to the method of Turek et al.,[46] and no change in either activity or selectivity could be observed.[47] It seems therefore that for low-iron-containing zeolites, the active sites responsible for the production of phenol are probably not only iron. Kustov et al. came to the same conclusions with an iron loading below 0.05 wt %.[17]

Catalytic Activity. Figure 1 shows a typical reaction profile for the catalytic reaction. Activity of different catalysts was compared after 70 min on stream. Figure 2 presents the results of conversion and selectivity for thermally and hydrothermally treated parent catalyst. Calcination at 973 K led to an enhanced catalytic activity. Zholobenko et al. explained this effect by the formation of structural defects, acting as active centers for α-oxygen formation.[48,49] Recently, Fraissard et al. have shown by a ^{129}Xe NMR study the ability of the ZSM-5 lattice to create an O-vacancy after severe thermal treatments.[50] Since coordinatively unsaturated aluminum appears in these structural defects, there is a relationship between these assumptions and Lewis acid-sites as active centers for N_2O activation. A further increase in the catalytic activity was observed after a mild steaming of 3 h. Steaming for 14 h led to a selectivity enhancement, with no further increase in benzene conversion. This indicates that after longer steaming procedures, the dealumination process stops (no EFAl created). These results are in agreement with those from Hölderich et al., who found a direct correlation between the amount of EFAl species and the phenol formation.[15,16]

TABLE 2: Catalytic Activity for the Different Chemically Modified Catalysts

sample	X_{Be}	S_{Ph}	sample	X_{Be}	S_{Ph}
Zeochem	21	70	TEOS	10.3	87
HCl-treated	10.6	72	H[F]-ZSM-5	5.2	21

Table 2 presents the results for the chemically modified catalysts. The HCl-treated catalyst showed a drastic decrease in the benzene conversion (from 21.0 to 10.6%), indicating that acid sites are directly involved in the reaction mechanism. In fact, this treatment is known to leach out Lewis acid sites and also to remove acid framework OH groups.[30,51]

The passivation of the outer surface (via TEOS treatment) led to a decrease in benzene conversion, together with an increase in the selectivity to phenol. This is mainly due to the decrease in carbon dioxide yield, from 5.5 to 1.5%, and thus in the suppression of the parallel pathway occurring on nonselective sites on the external surface of the zeolite. The selectivity improvement indicates that the phenol formation takes place inside the zeolite channels. Therefore, the characteristics of the ZSM-5 structure (channel size, confinement effects, strong acidity) have to be taken into account.

H[F]-ZSM-5 zeolite exhibited only low phenol yield (below 1%). The very low amount of BA of reduced strength could be an explanation. The low selectivity is due to CO_2 and dibenzofuran formation. The larger size of the crystals also favors consecutive reactions.

Figure 3 shows the influence of Brönsted acidity on this reaction. The Na^+-exchanged catalyst presents no catalytic activity at all (the ZSM-5 structure is preserved during the exchange procedure). It is consistent with this result to assume that Brönsted acidity is necessary for the catalysis of the reaction. However, this is a necessary condition but not

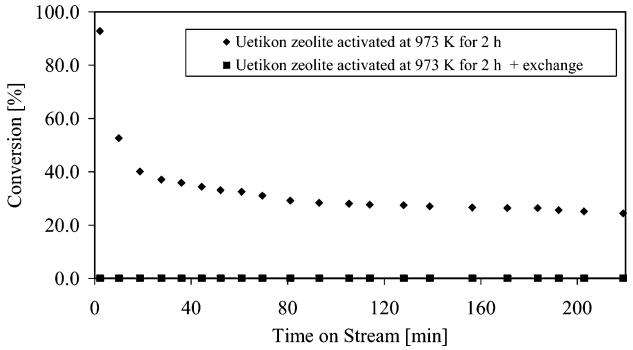

Figure 3. Evolution of benzene conversion with time on stream, for H-Zeochem and Na-exchanged catalysts.

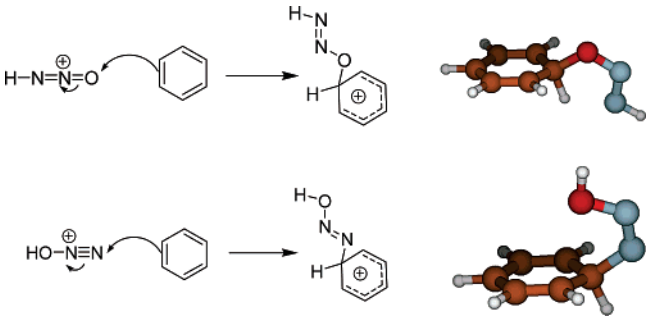

Figure 4. DFT geometries for the σ-complex resulting from electrophilic addition from the reaction of N- and O-protonated N_2O with benzene in the gas phase.

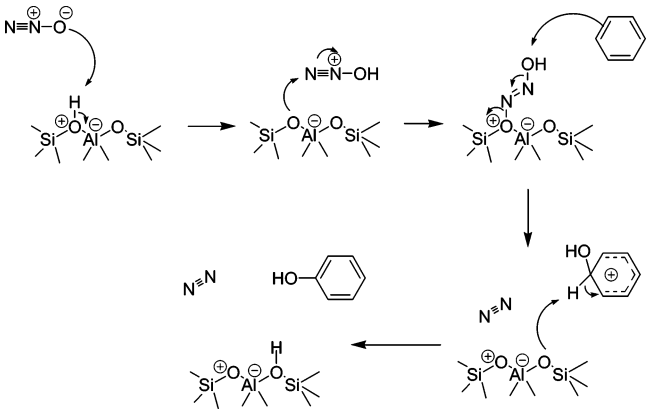

Figure 5. Possible mechanistic scheme for the participation of the zeolite active site in the reaction.

sufficient, since LA, exhibited by EFAl species (or iron or gallium in other cases), has been proven to be necessary for benzene partial oxidation.

DFT Calculations. To get a better understanding of the catalytic process, calculations using the density functional theory (DFT) were performed. At first the reaction of the protonated N_2O with benzene without considering the zeolite structure was studied, to have a better understanding about the reaction itself.

Calculations on the possibilities for the reaction of N_2O and N- or O-protonated N_2O with benzene were investigated at the B3LYP/6-31++G** level. Geometries of the species were optimized and energies of the several isomers were compared. All energy differences refer to enthalpy differences at 298 K and 1 atm. Differences in enthalpy do not usually change that much with temperature. Thus, despite the reaction being performed at 623 K, the conclusions made at 298 K can safely be extrapolated.

The DFT calculations show that protonation of N_2O is slightly preferred at the oxygen atom, this one being 1.8 kcal/mol more stable in relation to the protonation at the terminal nitrogen. These calculations are in agreement with those from Olah et al. devoted to the hydroxydiazonium ion.[65] The interaction of the protonated N_2O promotes the electrophilic attack on benzene, leading to the respective arenium ions, as shown in Figure 4. The reaction of N_2O protonated at the oxygen atom leads to the electrophilic attack by the nitrogen atom on the benzene. On the other way, protonation on the terminal nitrogen atom leads to addition through the oxygen atom, leading directly to a species that, upon deprotonation−reprotonation and N_2 loss steps, leads directly to a phenol molecule. If the ZSM-5 structure is considered, the only way for interaction of N_2O with the acid site was through the oxygen atom. Figure 5 shows a mechanism where N_2O first forms an intermediate that might be a model for the α-oxygen species and that does take into account benzene adsorption at this stage. However, detailed kinetics study have shown that both reactants are adsorbed on two active sites, thus following a Langmuir−Hinshelwood-type kinetics.[52,66]

To achieve a better understanding of the zeolite framework structure role in this reaction, we have performed additional calculations taking into account the zeolite pore. Those calculations were performed at the ONIOM (B3LYP/LANL2DZ:UFF/ZDO) level (see Computational Details for further information). In our cluster model used for these calculations (Figure 6) the atoms represented in the ball-and-stick model were computed at the DFT level, while the rest of the cavity was calculated at the molecular mechanics scheme using the UFF force field.

The adsorption mode of N_2O in H-ZSM5 was calculated to occur through the oxygen, due to a hydrogen bonding, as the O···H−O distance of 1.859 Å indicates (Figure 6). This adsorption is exothermic by 12.8 kcal/mol.

If we now consider the simultaneous adsorption of benzene and nitrous oxide and observe the resulting adsorption complex (Figure 7), it is possible to imagine that the attack can actually take place through direct displacement of N_2 from this complex (Figure 8). Hence, an epoxide-type of intermediate is formed, which can be further protonated and, through rearrangement, can lead to the products.

Figure 9 shows the structure of this epoxide, hydrogen bonded to the acid site of the H-ZSM-5. This complex shows that the epoxide is asymmetric, containing different C−O bond lengths (1.529 and 1.513 Å). This indicates a tendency to undergo ring cleavage after protonation of the epoxide ring, leading to a σ-complex, which eventually deprotonates, affording phenol (product) and regenerating the acid site. The further conversion of this complex into the phenol−H-ZSM-5 complex was calculated to be exothermic by 64.6 kcal/mol.

Figure 10 shows the structure of the PhOH−H-ZSM-5 complex. It is observed that phenol is bonded to the acid site through two hydrogen bonds. The further desorption of phenol from the acid site is calculated to be endothermic by 44 kcal/mol. It appears that the ZSM-5 structure is essential for this reaction. These calculations confirm that N_2O can be activated at one side of the cavity, while benzene could be adsorbed at the other side as a π-complex. Due to the relatively small cavity size in ZSM-5 (the maximum diameter of a sphere that can be included in the framework is 6.3 Å), these two species are therefore favorably oriented toward each other. This effect due to the fit between the size of the reactants (and the resulting complex) and the aperture of the channel is then the key point for the reaction to take place, since it helps the reaction from the entropic point of view.

While trying to make a parallelism with the work done in liquid superacids by the group of Olah,[3,5] another possibility could be the formation of the HO-ZSM-5 acid site, i.e., an electrophilic hydroxyl group bonded to the zeolite framework, forming a kind of hydroperoxide acid site (Figure 12). This can be a source of electrophilic hydroxyl groups, which favors benzene oxidation to phenol. Figure 11 shows the optimized structure for the adsorption complex between benzene and HO-ZSM-5. The benzene adsorption energy is calculated to be of −29.4 kcal/mol.

Figure 12 presents the mechanistic scheme that involves such a "peroxo-type" of acid site.

Reaction Mechanism: Superacid-Catalyzed Activation? In a recent publication devoted to the kinetics of this reaction,[52] we have shown that both benzene and nitrous oxide are adsorbed on two different acid sites. The partial order of reaction with

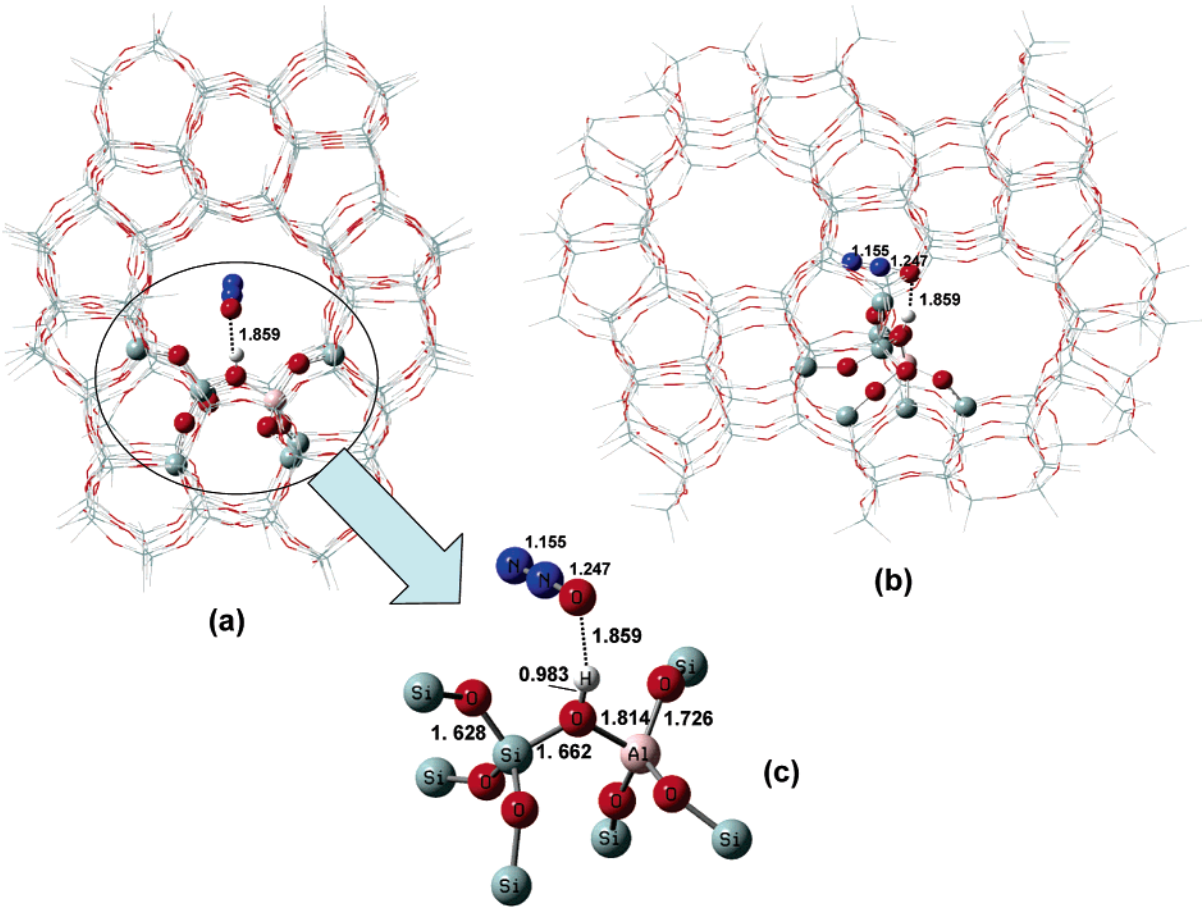

Figure 6. Adsorption of N_2O in the zeolite active sites. Views a and b show the cluster T200 through the channels (high-level ONIOM atoms as balls-and-sticks and lower level showed in wireframe). View c shows details of the acid site, with the rest of zeolite structure omitted for clarity purposes.

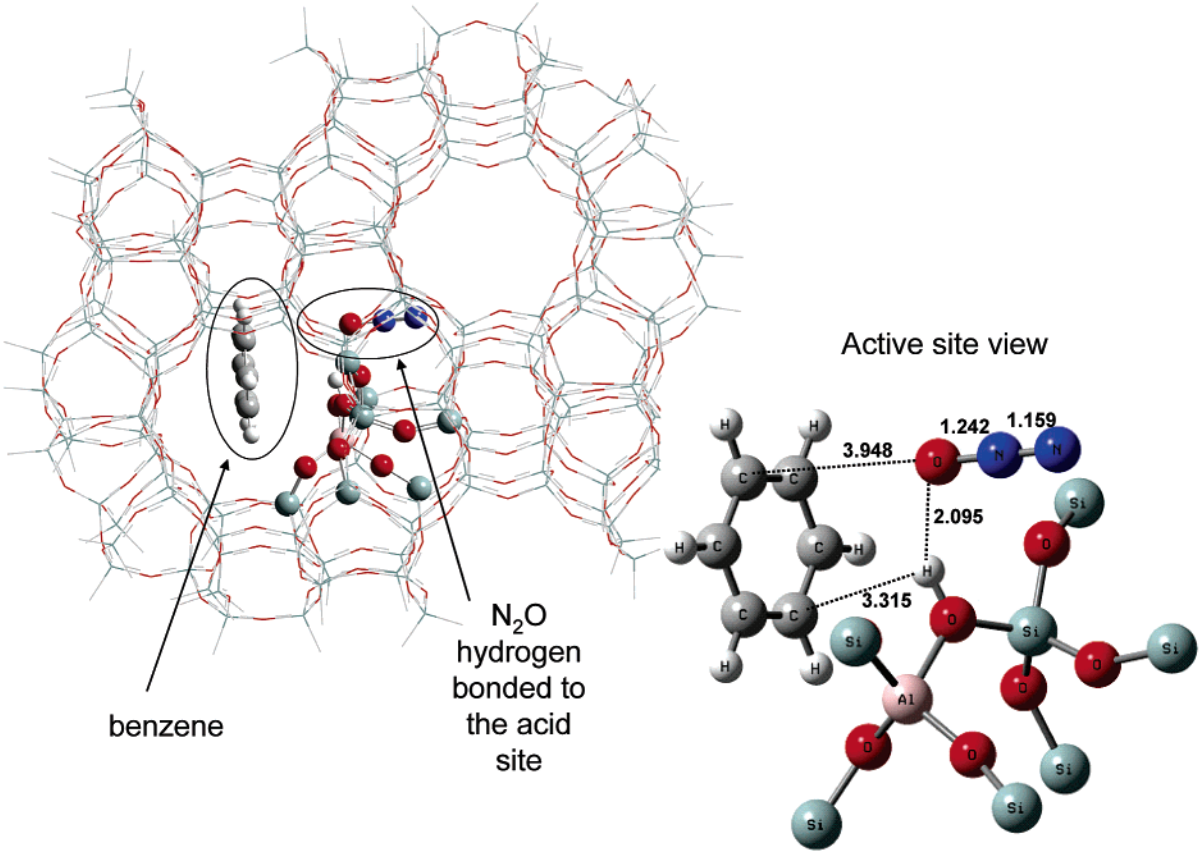

Figure 7. Detailed view of the simultaneous adsorption of benzene in the N_2O·H-ZSM-5 π-complex.

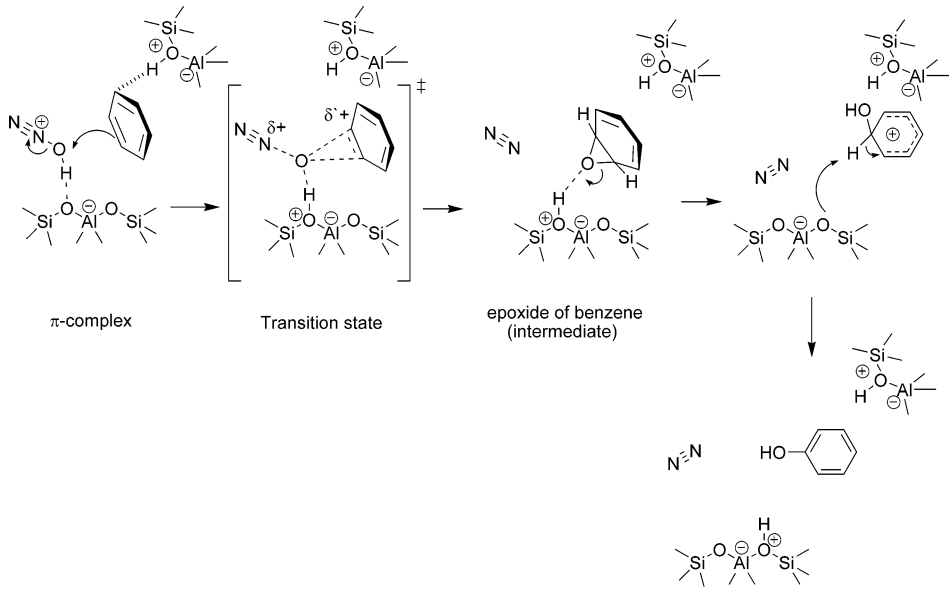

Figure 8. Proposed mechanistic scheme for benzene hydroxylation, through direct displacement and with an epoxide intermediate.

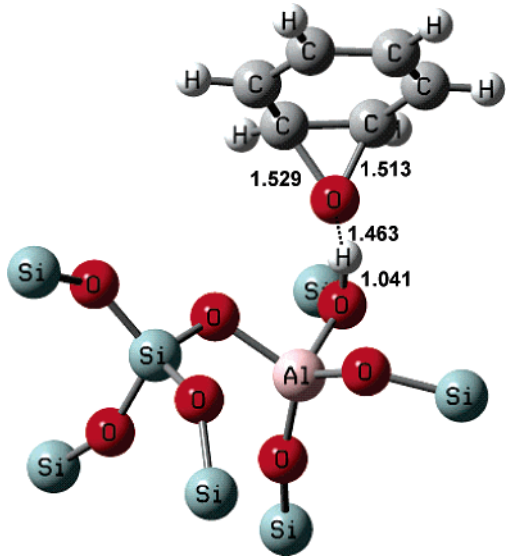

Figure 9. Hydrogen-bonded complex between an epoxide of benzene and H-ZSM-5. The zeolite structure was omitted for clarity.

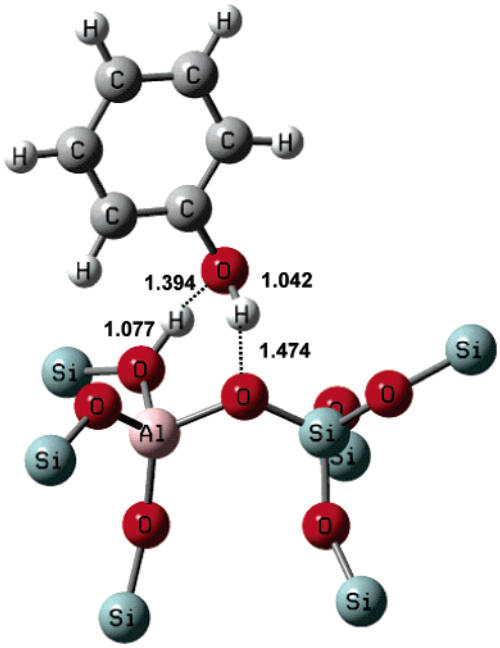

Figure 10. Hydrogen-bonded complex between phenol and H-ZSM-5. The zeolite structure was omitted for clarity.

respect to N_2O was close to zero, indicating an extremely fast saturation of all the active sites at low N_2O concentration. In other words, the amount of acid sites necessary to activate nitrous oxide is limited. The adsorption of benzene occurs on an acid site, which should be in the vicinity of the one that activates nitrous oxide.[26] The DFT calculations of the present study tend to confirm the key role of acid sites, but in a peculiar spatial arrangement (Figures 10 and 11). Furthermore, the three-dimensional H-ZSM-5 is known to exhibit a very strong acidity equivalent to a 70% solution of sulfuric acid.[53] Therefore, the participation of the Brönsted acid sites of the ZSM-5 structure seems reasonable[7−9,54]. Haw and co-workers have demonstrated by H/D exchange and theoretical investigations an interaction between benzene and bridging OH groups[37,55−57] forming a π-complex species. It is possible that these complexes can also be formed on Lewis acid sites. Recently, Reitzmann et al. have shown via a transient (multipulse) adsorption of N_2O over iron-doped ZSM-5 that the mode of adsorption differs from the non-iron-promoted H-ZSM-5.[67,68] These authors came to the conclusions that other active sites than exclusively iron species are involved.[68]

Carbenium ion-like species are stabilized within the zeolitic framework via interaction with two oxygens.[36] Zeolites are not true superacids at room temperature,[39] but they can mimic them by diminishing the energy-barrier toward the carbenium ion. Confinement effects in the pores by the long-range electrostatic field[29,32−34] should permit the absorption of benzene and N_2O molecules in the solid solvent and guide them toward the strong acid sites. However, the π-complex between benzene and the acid site is the most stable configuration of this system. The protonation of the N_2O by either the EFAL or framework acid sites, followed by its adsorption into the zeolitic structure, could afford an adsorbed species with the ability to undergo further electrophilic attack by the benzene adsorbed on the surface as a π-complex, leading to a bimolecular mechanism (Figure 5).

Following our previous kinetics study,[52] these experimental results together with DFT calculations led us to assume that an electrophilic substitution on the aromatic ring by an electrophilic species occurs. The existence of superelectrophiles in zeolites

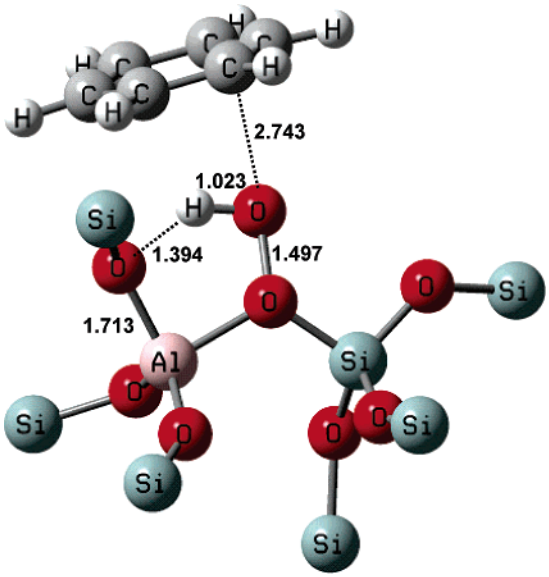

Figure 11. Adsorption complex between benzene and HO-ZSM-5. The zeolite structure was omitted for clarity.

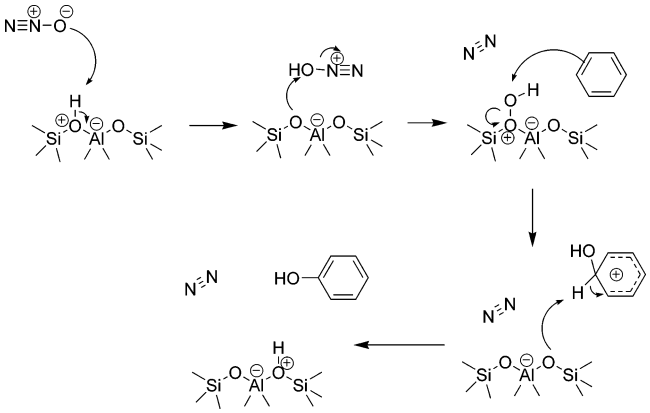

Figure 12. Mechanistic scheme involving the formation of a hydroxyl group bonded to the zeolite surface (HO-ZSM-5) and its further attack on benzene.

has been recently proposed.[58−59] The confinement effects that considerably enhance the van der Waals interactions within the framework also support this Langmuir−Hinshelwood mechanism.[32] The following question arises: Is it statistically reasonable to have an Al-pairing in the same unit cell? Derouane and Fripiat have shown by quantum chemical calculations that the pairing of Al in the ZSM-5 structure is favored as an Al−O−Si−O−Al linkage.[60] Statistical studies also confirmed the relatively high probability for having a second Al in the NNN coordination spheres.[61−63] Notte has already proposed that an optimum should be found between the amount of extraframework species and Brönsted sites.[26] A specific spatial geometry (Figures 10 and 11) between the protonic acid sites and EFAl is created through the mild steaming procedure[64] that led to improve catalytic activity. These interactions can create specific "superacid-sites" or more precisely "perfectly tailored sites" able to selectively activate benzene and N_2O for phenol formation.

Conclusion

This study shows the primary importance of Brönsted acid sites in the gas-phase benzene hydroxylation by N_2O. Those sites work in combination with the Lewis acidity: EFAl species present in the vicinity of framework Al.

Our previous Langmuir−Hinshelwood model,[52] supposing a most abundant surface intermediate (MASI), and the present data consistently point out the coexistence of two neighboring acid-sites. Therefore an acid-catalyzed mechanism is proposed, passing through a Wheland-type intermediate stabilized within the zeolite framework to explain the particular behavior of benzene and nitrous oxide inside the MFI structure.

Since, the confinement effects are very important in the ZSM-5 zeolite, especially for benzene molecules, the size of which fits the size of the channel aperture, the shape-selectivity is also a key parameter for performing this reaction.

Computational Details

Full geometry optimizations for all structures were performed with the Gaussian03W package[69] using density functional theory (DFT) and were characterized as minima on the potential energy surface by the absence of imaginary frequencies after vibrational analysis. The cluster used for simulating the ZSM-5 structure in the calculations contains 199 silicon atoms and one aluminum atom, affording a total of 200 tetrahedral atoms (T200). The large unit cell of ZSM-5 (288 atoms) does not allow full ab initio periodic calculations. For this reason, a two-layer ONIOM method[70] was used for the calculations, at the B3LYP/LANL2DZ:UFF/ZDO level. The ONIOM method has been shown to give good results in the study of reactions in zeolite structures.[71] The zeolite clusters were cut out from the crystallographic structure of ZSM-5.[72] The active site was calculated at the higher level (B3LYP/LANL2DZ) and consisted of the acid site SiO(H)Al, with the surrounding next neighboring silicon atoms (cluster T8) and the substrates. The rest of the structure, corresponding to a cluster T192, was treated at a lower level with the UFF force field. Outer dangling bonds in the lower level, which in the authentic zeolite would connect the cluster with the rest of the solid, were saturated with hydrogen atoms. Zygmunt et al.[73] studied the applicability of various readily available functionals for studying molecular adsorption in small zeolite clusters and found that the B3LYP functional is the best choice for DFT treatment of small zeolite clusters. The T200 model is considered to be large enough to cover all important framework effects on both the active site and the adsorbate. A single Si/Al substitution was considered, located at the intersection of the main and sinusoidal channels, into a site accessible to adsorbates (crystallographic site Al1−O21(H)−Si5, numbered as in ref 72).

Acknowledgment. The authors gratefully acknowledge Mr. E. Casali for technical assistance in the catalyst characterization, Zeochem (Uetikon, Switzerland) for kindly providing their zeolites and FAPERJ and CNPq for financial support.

References and Notes

(1) Hölderich, W. F. In New reactions in various fields and production of specialty chemicals. *Proceedings of the 10th International Congress on Catalysis*; Amsterdam, Elsevier Science Publishers B. V., 1993; pp 127−163.

(2) Hölderich, W. F.; van Bekkum, H. *Stud. Surf. Sci. Catal.* **1991**, *58*, 631.

(3) Olah, G. A.; Ohnishi, R. *J. Org. Chem.* **1978**, *43*, 865.

(4) Sheldon, R. A. *ChemTech* **1991**, 566−577.

(5) Yoneda, N.; Olah, G. A. *J. Am. Chem. Soc.* **1977**, *99*, 3113.

(6) Iwamoto, M.; Hirata, J.; Matsukami, K.; Kagawa, S. *J. Phys. Chem.* **1983**, *87*, 903−905.

(7) Suzuki, E.; Nakashiro, K.; Ono, Y. *Chem. Lett.* **1988**, 953−956.

(8) Burch, R.; Howitt, C. *Appl. Catal. A* **1992**, *86*, 139−146.

(9) Gubelmann, M.; Tirel, P. J. US Patent 5,001,280, 1991.

(10) Panov, G. I.; Kharitonov, A. S.; Sobolev, V. I. *Appl. Catal. A* **1993**, *98*, 1−20.

(11) Panov, G. I. *Cattech* **2000**, *4*, 18−32.

(12) Panov, G. I.; Uriarte, A. K.; Rodkin, M. A.; Sobolev, V. I. *Catal. Today* **1998**, *41*, 365−385.

(13) Panov, G. I.; Sobolev, V. I.; Dubkov, K. A.; Kharitonov, A. S. *Stud. Surf. Sci. Catal.* **1996**, *101*, 493−502.
(14) Motz, J. L.; Heinichen, H.; Hölderich, W. F. *J. Mol. Catal. A* **1998**, *136*, 175−184.
(15) Motz, J. L.; Heinichen, H.; Hölderich, W. F. *Stud. Surf. Sci. Catal.* 1997, *105B*, 1053−1060.
(16) Hölderich, H.; Motz, J. L.; Heinichen, H. German Patent DE 19,-634,406, 1998.
(17) Kustov, L. M.; Tarasov, A. L.; Bogdan, V. I.; Tyrlov, A. A.; Fulmer, J. W. *Catal. Today* 61 **2000**, 123−128.
(18) Wang, Q. L.; Giannetto, G.; Guisnet, M. *J. Catal.* **1991**, *130*, 471−482.
(19) Sendoda, Y.; Ono, Y. *Zeolites* **1988**, *8*, 101−105.
(20) Lago, R. M.; Haag, W. O.; Mikovsky, R. J.; Olson, D. H.; Hellring, S. D.; Schmitt, K. D.; Kerr, G. T. *Stud. Surf. Sci. Catal.* **1986**, *28*, 677−684.
(21) Kumar, S.; Sinha, A. K.; Hegde, S. G.; Sivasanker, S. *J. Mol. Catal. A* **2000**, *154*, 115−120.
(22) Freude, D.; Ernst, H.; Mildner, T.; Pfeifer, H.; Wolf, I. *Stud. Surf. Sci. Catal.* **1993**, *90*, 105−116.
(23) Datka, J.; Marschmeyer, S.; Neubauer, T.; Meusinger, J.; Papp, H.; Schütze, F. W.; Szpyt, I. *J. Phys. Chem.* **1996**, *100*, 14451−14456.
(24) Biaglow, A. I.; Parrillo, D. J.; Kokotailo, G. T.; Gorte, R. J. *J. Catal.* **1994**, *148*, 213−223.
(25) Lónyi, F.; Lunsford, J. H. *J. Catal.* **1992**, *136*, 566−577.
(26) Notte, P. P. *Topic. Catal.* **2000**, *13*, 387−394.
(27) Mirodatos, C.; Barthomeuf, D. *J. Chem. Soc. Chem. Commun.* **1981**, 39.
(28) Dubkov, K. A.; Ovanesyan, N. S.; Shteinman, A. A.; Starokon, E. V.; Panov, G. I. *J. Catal.* **2002**, *207*, 341−352.
(29) Zicovich-Wilson, C. M.; Corma, A.; Viruela, P. *J. Phys. Chem.* **1994**, *98*, 10863−10870.
(30) Haouas, M.; Kogelbauer, A.; Prins, R. *Catal. Lett.* **2000**, *70*, 61−65.
(31) Fraissard, J. *Stud. Surf. Sci. Catal.* **1980**, *5*, 343.
(32) Derouane, E. G.; Chang, C. D. *Microporororous Mesopororous Mater.* **2000**, *35*−*36*, 425−433.
(33) Corma, A. *Stud. Surf. Sci. Catal.* **1995**, *94*, 736−747.
(34) Barthomeuf, D. *Stud. Surf. Sci. Catal.* **1997**, *105C*, 1677−1706.
(35) Chang, C. D.; Xiong, Y.; Rodewald, P. G. *J. Am. Chem. Soc.* **1995**, *117*, 9427−9431.
(36) Esteves, P. M.; Mota, C. J. A.; Ramirez-Solis, A.; Hernandez-Lamoneda, R. *Topic. Catal.* **1998**, *6*, 163−168.
(37) Haw, J. F.; Nicholas, J. B.; Xu, T.; Beck, L. W.; Ferguson, D. B. *Acc. Chem. Res.* **1996**, *29*, 259.
(38) Nicholas, J. B. *Topic. Catal.* **1998**, *6*, 181−189.
(39) Olah, G. A.; Prakash, G. K. S.; Sommer, J., *Superacids*; Wiley: New York, 1985.
(40) Louis B.; Kiwi-Minsker L. *Microporororous Mesopororous Mater.* **2004**, *74*, 171.
(41) Müller, M.; Harvey, G.; Prins, R. *Microporous Mesoporous Mater.* **2000**, *34*, 135−147.
(42) Koller, H.; Wölker, A.; Eckert, H.; Panz, C.; Behrens, P. *Angew. Chem., Int. Ed. Engl.* **1997**, *36*, 2823−2825.
(43) Fyfe, C. A.; Brouwer, D. H.; Lewis, A. R.; Chezeau, J. M. *J. Am. Chem. Soc.* **2001**, *123*, 6882−6891.
(44) Pirutko, L. V.; Chernyavsky, V. S.; Uriarte, A. K.; Panov, G. I. *Appl. Catal. A* **2002**, *227*, 143−157.
(45) Sobolev, V. I.; Panov, G. I.; Kharitonov, A. S.; Paukshtis, Ye. A. *J. Mol. Catal.* **1993**, *84*, 117−124.
(46) Kögel, M.; Mönnig, R.; Schwieger, W.; Tissler, A.; Turek, T. *J. Catal.* **1999**, *182*, 470.
(47) Louis, B., Ph.D. Thesis, Ecole Polytechnique Federale de Lausanne, no. 2651, 2002, Lausanne, Switzerland.
(48) Zholobenko, V.; Senchenya, I. N.; Kustov, L. M.; Kazansky, V. B. *Kinet. Catal.* **1991**, *32*, 132.
(49) Zholobenko, V. *Mendeleev Commun.* **1993**, 28−29.
(50) Balint, I.; Springel-Huet, M.-A.; Aika K−I.; Fraissard, J. *Phys. Chem. Chem. Phys.* **1999**, *1*, 3845−3851.
(51) Barthomeuf, D. *Mater. Chem. Phys.* **1987**, *17*, 49−71.
(52) Louis, B.; Kiwi-Minsker, L.; Reuse, P.; Renken, A. *Ind. Eng. Chem. Res.* **2001**, *40*, 1454−1459.
(53) Xu, T.; Munson, E. J.; Haw, J. F. *J. Am. Chem. Soc.* **1994**, *116*, 1962.
(54) Burch, R.; Howitt, C. *Appl. Catal.* **1993**, *106*, 167−183.
(55) Beck, L. W.; Xu, T.; Nicholas, J. B.; Haw, J. F. *J. Am. Chem. Soc.* **1995**, *117*, 11594.
(56) White, J. L.; Beck, L. W.; Haw, J. F. *J. Am. Chem. Soc.* **1992**, *114*, 6182.
(57) Xu, T.; Barich, D. H.; Goguen, P. W.; Song, W.; Wang, Z.; Nicholas, J. B.; Haw, J. F. *J. Am. Chem. Soc.* **1998**, *120*, 4025−4026.
(58) Klumpp, D. A.; Rendy, R.; McElrea, A. *Tetrahedron Lett.* **2004**, *45*, 7959.
(59) Koltunov, K. Y.; Walspurger, S.; Sommer, J. *Catal. Lett.* **2004**, *98*, 89.
(60) Derouane, E. G.; Fripiat, J. G. *Zeolites* **1985**, *5*, 165.
(61) Goodman, B. R.; Haas, K. C.; Schneider, W. F.; Adams, J. B. *Catal. Lett.* **2000**, *68*, 85−93.
(62) Dédecék, J.; Kaucky, D.; Wichterlová, B. *Chem. Commun.* **2001**, 970−971.
(63) Rice, M. J.; Chakraborty, A. K.; Bell, A. T. *J. Catal.* **1999**, *186*, 222−227.
(64) Brunner, E.; Ernst, H.; Freude, D.; Fröhlich, T.; Hunger, M.; Pfeifer, H. *J. Catal.* **1991**, *127*, 34−41.
(65) Olah, G. A.; Herges, R.; Laali, K.; Segal, G. A. *J. Am. Chem. Soc.* **1986**, *108*, 2054−2057.
(66) Reitzmann, A.; Klemm, E.; Emig, G. *Chem. Eng. J.* **2002**, *90*, 149−164.
(67) Ates, A.; Reitzmann, A. *React. Kinet. Catal. Lett.* **2005**, *86*, 11−20.
(68) Ates, A.; Reitzmann, A. *J. Catal.* **2005**, *235*, 164−174.
(69) Frisch, M. J.; Trucks, G. W.; Schlegel, H. B.; Scuseria, G. E.; Robb, M. A.; Cheeseman, J. R.; Montgomery, J. A., Jr.; Vreven, T.; Kudin, K. N.; Burant, J. C.; Millam, J. M.; Iyengar, S. S.; Tomasi, J.; Barone, V.; Mennucci, B.; Cossi, M.; Scalmani, G.; Rega, N.; Petersson, G. A.; Nakatsuji, H.; Hada, M.; Ehara, M.; Toyota, K.; Fukuda, R.; Hasegawa, J.; Ishida, M.; Nakajima, T.; Honda, Y.; Kitao, O.; Nakai, H.; Klene, M.; Li, X.; Knox, J. E.; Hratchian, H. P.; Cross, J. B.; Bakken, V.; Adamo, C.; Jaramillo, J.; Gomperts, R.; Stratmann, R. E.; Yazyev, O.; Austin, A. J.; Cammi, R.; Pomelli, C.; Ochterski, J. W.; Ayala, P. Y.; Morokuma, K.; Voth, G. A.; Salvador, P.; Dannenberg, J. J.; Zakrzewski, V. G.; Dapprich, S.; Daniels, A. D.; Strain, M. C.; Farkas, O.; Malick, D. K.; Rabuck, A. D.; Raghavachari, K.; Foresman, J. B.; Ortiz, J. V.; Cui, Q.; Baboul, A. G.; Clifford, S.; Cioslowski, J.; Stefanov, B. B.; Liu, G.; Liashenko, A.; Piskorz, P.; Komaromi, I.; Martin, R. L.; Fox, D. J.; Keith, T.; Al-Laham, M. A.; Peng, C. Y.; Nanayakkara, A.; Challacombe, M.; Gill, P. M. W.; Johnson, B.; Chen, W.; Wong, M. W.; Gonzalez, C.; Pople, J. A. *Gaussian 03W*, Revision B.03; Gaussian, Inc.: Wallingford, CT, 2003.
(70) Dapprich, S.; Komaromi, I.; Byun, K. S.; Morokuma, K.; Frisch, M. J. *J. Mol. Struct. (THEOCHEM)* **1999**, *461* 1.
(71) Solans-Monfort, X.; Sodupe, M.; Branchadell, V.; Sauer, J.; Orlando, R.; Ugliengo, P. *J. Phys. Chem. B* **2005**, *109*, 3539.
(72) Olson D. H.; Kokotallo, G. T.; Lawton, S. L.; Meier, W. M. *J. Phys. Chem.* **1981**, *85*, 2238−2243.
(73) Zygmunt, S. A.; Mueller, R. M.; Curtiss, L. A.; Iton, L. E. *J. Mol. Struct.(THEOCHEM)* **1998**, *430*, 9.